Machine learning based pulse characterisation in figure-eight mode-locked lasers

ALEXEY KOKHANOVSKIY[1,*], ANASTASIA BEDNYAKOVA[1,2], EVGENY KUPRIKOV[1], ALEKSEY IVANENKO[1], MIKHAIL DYATLOV[1], DANIIL LOTKOV[1], SERGEY KOBTSEV[1], AND SERGEY TURITSYN[1,3]

[1] *Division of Laser Physics and Innovative Technologies, Novosibirsk State University, Pirogova str., 2, Novosibirsk, 630090, Russia*
[2] *Institute of Computational Technologies SB RAS, Novosibirsk, 630090, Russia*
[3] *Aston Institute of Photonic Technologies, Aston University, B4 7ET, Birmingham, UK*
[*] *Corresponding author: alexey.kokhanovskiy@gmail.com*

Compiled August 15, 2019

By combining machine learning methods and the dispersive Fourier transform we demonstrate, to the best of our knowledge, for the first time a possibility to determine the temporal duration of picosecond-scale laser pulses using nanosecond photodetector. A fiber figure of eight (F-8) laser with two amplifiers in a resonator was used to generate pulses with duration varying from 28 to 160 ps and spectral width varied in the range of 0.75 to 12 nm. Average power of the pulses was in range from 40 to 300 mW. The trained artificial neural network makes it possible to predict the pulse duration with the mean agreement of 95%. The proposed technique paves the way to creating compact and low cost feedback for complex laser systems.

OCIS codes: (230.4320) Nonlinear optical devices; (160.4760) Optical properties;(190.4360) Nonlinear optics, devices; (060.4370) Nonlinear optics, fibers;(190.5530) Pulse propagation and temporal solitons;

http://dx.doi.org/10.1364/ao.XX.XXXXXX

1. INTRODUCTION

One of the modern trends in development of mode-locked fiber lasers is a focus on precise adjustment of temporal and spectral properties of optical pulses [1–4] at the expense of increasing complexity of system design. The resulting large number of cavity parameters defining laser performance requires new approaches to controlling them. From this view point, the machine learning based techniques are attractive for control and management of complex laser systems. Machine learning algorithms have been already used for optimization of laser performance [5], self-starting [6] and adjustment of system parameters to environmental changes [7].

Key part of any self-adjusting laser system is a feedback loop which links together laser performance and variable laser cavity parameters. In general, experimental realization of such feedback system requires a set of measurement devices and (desirably) electronically controlled feedback to laser cavity parameters. To optimize performance of electronically controlled mode-locked fiber laser based on nonlinear polarization evolution four devices were used: autocorrelator, optical and radiofrequency analyzers, oscilloscope [5, 6]. In fiber laser with spatial light modulator autocorrelator and optical analyzer formed a feedback system to generate 40 fs pulses [1]. Laser performance could be also optimized outside its cavity, for example, by pulse compressor that requires frequency – resolved optical gating measurement as a feedback response [8]. To sum up, the common way to create a feedback for adaptive fiber lasers is to use optical spectrum analyzer, oscilloscope and autocorrelator(or other device measuring duration of ultra-short pulses) as measurement setups. These devices provide information about basic pulse parameters: optical spectrum, time duration, repetition rate, average power, energy and peak power. In principle, pulse has to be measured in both time and frequency domains because of nontrivial relation between optical spectrum and time envelope of the pulse [9].

A large set of tools leads to complexity and corresponding cost of the controlled devices that greatly limit application of the emerging feedback based approaches to laboratory experiments. Reduction in the number of measurement tools and devices required for realization of feedback loop is a critical challenge in development of "smart" laser systems. In broader perspective, first attempt to reduce the number of measurement setups was made in [10], where neural network predicts pulse parameters of x-ray free electron laser.

The novelty of our work is an experimental demonstration of a feedback system that requires nanosecond detector to measure all listed basic parameters of a picosecond pulse. We implement this novel technique using the following steps using acquisition of an oscilloscope trace. First, registration of time-domain comb of pulses indicates the mode-locking regime. Second, Fourier transform of oscilloscope trace provides information about radio-frequency spectrum of the mode-locked regime and, consequently, about a quality of mode-locking. And finally, dispersive Fourier transform (DFT) analysis available from the oscilloscope trace of dispersively stretched pulses, allows one to measure optical spectrum of the pulses [11]. We would like to stress that oscilloscope trace of short optical pulses does not give directly any information about their duration. Sensitivity of photodetector is limited by its relaxation time, which makes

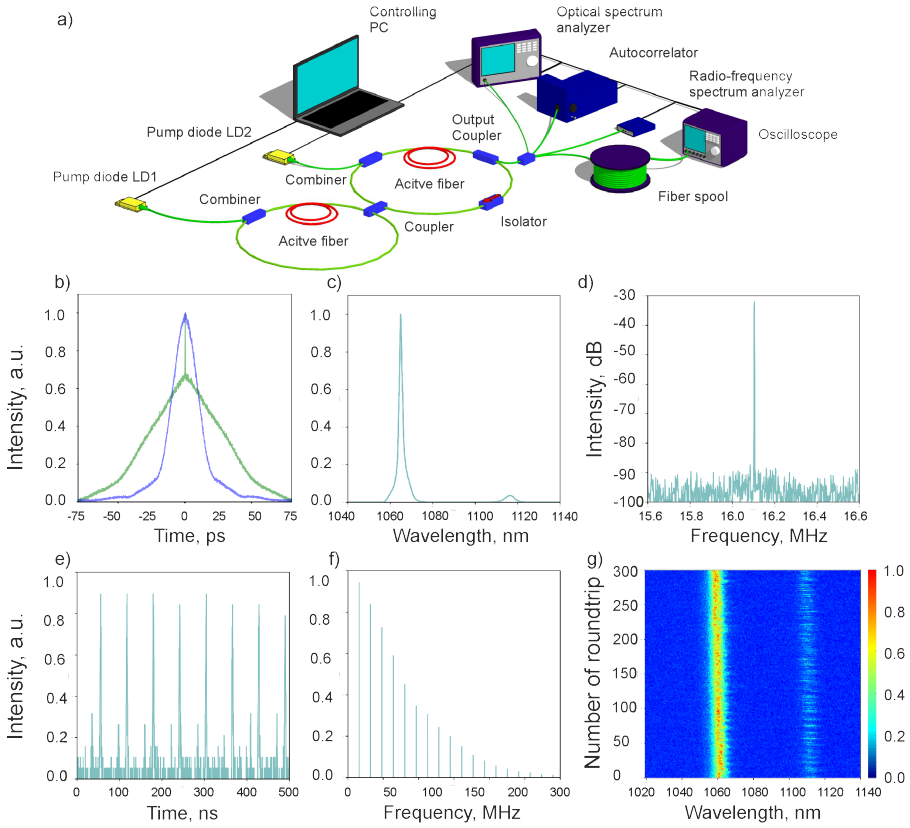

Fig. 1. (a) Experimental setup. (b) ACF examples of coherent (blue line) and noise-like (green line) output pulses. (c) Example of optical spectrum of a pulse with significant Raman part. (d) Example of radio-frequency spectrum of a pulse comb near fundamental mode of a laser cavity. (e) Oscilloscope trace of a pulse comb detected after propagation through long spool of a fiber. (f) Fourier transformation of oscilloscope trace representing radio-frequency spectrum of DFT pulse comb. (g) Dispersive Fourier transformation of a pulse comb presenting optical spectrum of a pulse per roundtrip.

impossible to measure duration of optical pulses less than hundreds of picoseconds.

The goal of this work is to demonstrate a feasibility of measurement of the temporal characteristics of the output pulses of F-8 fiber laser employing DFT trace of pulse comb and machine learning technique. To determine temporal width of pulses we used machine learning techniques focusing on artificial neural network. We demonstrate the general approach using as an example the F-8 fiber lasers with two amplifiers where a large number of pulse regimes with different spectral and temporal characteristics can be observe. We believe that our findings pave the way to implement compact and relatively low cost feedback loop for laser systems.

2. EXPERIMENT

Figure 1(a) illustrates the F-8 mode-locked fiber laser under study. The laser cavity consists of two fiber loops, unidirectional (main) and bidirectional (nonlinear amplifying loop mirror) ones, connected to each other by a 40/60 coupler. The main loop includes 70% output coupler and a high-power Faraday isolator that provides unidirectional propagation. Both loops comprise 2.5-m long amplifying sections of double-clad Yb-doped fibers with absorption of 3.9 dB/m at 978 nm. Active fibers are pumped through fiber beam combiners by independently controlled multimode laser diodes with an optical power of up to 4.5 W at a wavelength of 978 nm. The fibers inside the cavity, both passive and active, are polarization-maintaining.

To measure basic parameters of the mode-locked pulse such as time duration, optical spectrum and radio-frequency spectrum the following tools were used: the A.P.E. pulseCheck autocorrelator with scanning range from 120 fs up to 160 ps, Tektronix RSA 3308B radio-frequency spectrum analyzer with 2-Hz resolution for inter-mode beat signal measuring, the Yokogawa AQ 6375 optical spectrum analyzer (OSA) with resolution 0.1 nm, the Tektronix DPO71604C oscilloscope connected with photo detector with bandwidth of 1 GHz.

A full-width half maximum of autocorrelation function (ACF) was used as a measure of pulse duration. ACF duration of generated pulses varied from 28 to 160 ps. To distinguish single-scale (coherent) and double-scale (noise-like) pulses we also measure a contrast of ACF coherence spike (Fig. 1 (b)). The contrast of coherence spike was calculated as a difference between a height of coherence spike and a height of ACF envelope of normalized ACF trace. To derive the height of ACF envelope, we applied to ACF trace the low-pass 3-order Butterworth filter with 0.01 (π rad/sample) cut-off frequency. For example, the contrast of ACF coherence spike of a noise-like pulse shown in Fig. 1 (b) (green line) is 0.32. Contrast of coherence spike varied from 0.0036 to 0.5. We assume that noise-like pulses have coherence spike contrast higher than 0.02. Optical spectrum of mode-locked pulses generated by the fiber laser includes two parts, corresponding to signal pulse and noisy Raman pulse (Fig. 1 (c)). Both pulses were characterized by average power and spectrum width. For the signal part, these values ranged between 40 and 300 mW

and 0.75 and 12 nm respectively. The average power of Raman ranged between 0 and 35 % of total power. The signal to noise ratio of radio-frequency inter-mode beats (RF contrast in RF maps) was measured as a contrast between the background level and the spike at fundamental frequency (Fig. 1 (d)). The RF-contrast varied between 0 and 73 dB.

In this work we aim to replace these three measurement tools by a single oscilloscope that measures DFT trace of optical pulses. To measure DFT trace of optical pulses we used 14.93-km-long fiber span with dispersion β_2 = 15.1e-27 s^2/m. Stretched pulses were measured by the oscilloscope with the sampling rate of 3 GS/s (Fig. 1 (e)). Some pulse parameters such as radio-frequency and optical spectrum can be measured directly from DFT trace. Fourier transformation of DFT trace gives radio-frequency spectrum of a pulse comb (Fig. 1 (f)). Using obtained radio-frequency spectrum we calculated number, average power and standard deviation of radio-frequency peaks. Rescaling DFT trace provides optical spectrum of pulses per roundtrip (Fig. 1 g), and therefore gives similar information as optical spectrum analyzer.

The most challenging part was to determine temporal duration of a pulse. In fact, there is no direct relation between its optical or radio-frequency spectrum and time duration. However, laser system with specific chromatic dispersion, nonlinear coefficient and Stokes shift generates specific set of pulsed regimes and, therefore, there is no need to make a universal measurement tool to determine pulse parameters. In this work we demonstrate that it is possible to train artificial neural network to determine with acceptable accuracy a temporal duration of the pulses by following features extracted from DFT trace: (i) optical spectral width of signal, (ii) optical spectral width of Raman pulse, (iii) optical power of signal, (iv) optical power of Raman pulse, (v) total optical power, (vi) number of radio-frequency spectrum peaks, (vii) average power of radio-frequency spectrum peaks, (viii) standard deviation (std) of radio-frequency peaks power.

It worth to mention that direct measuring of optical spectrum of a pulse using DFT setup requires careful adjusting of input power to reduce influence of nonlinear effects such as self-phase modulation and Raman scattering. We would have to implement a variable attenuator to control input power and measure optical spectrum width of the pulses with average powers from 40 to 300 mW. Instead of using an attenuator we apply artificial neural network to predict a width of optical spectrum at the laser output, assuming nonlinear dependency between the spectra width at the DFT line input and output.

3. MACHINE LEARNING APPROACH

At the first stage we estimate ACF width for the whole variety of generated optical pulses, including partially coherent double-scale pulses. Artificial neural network (ANN) model from TensorFlow software library [12] was employed to determine full-width-half-maximum (FWHM) of the ACF trace. The ANN is comprised of 3 hidden layers with 32, 32, and 16 neurons. For the training of ANN, a data set containing 13600 examples was used. To obtain data, we continuously changed the powers of both pumping diodes in the range from 4.5 to 0.5 W in the following order. At a fixed power of the LD1, we gradually reduced the power of the LD2 from 4.5 to 0.5 W with a step of 0.03 W and measured the parameters of the output radiation at each power step. Then the power of LD1 was reduced by 0.03 W and the procedure was repeated until LD1 power became equal to 0.5 W. Eight parameters extracted from DFT trace were used as features for estimate: signal and Raman powers, spectral width of signal and Raman pulses, number and average power of radio-frequency spectrum peaks, standard deviation and normalized standard deviation of the radio-frequency peaks power. Note, that we were keeping only the variables showing a high correlation with the target characteristics. Instead of normalization of the features we used batch normalization layer before each nonlinear layer of the network. We also removed outliers in the outputs, corresponding to continuous-wave generation, unstable generation of fully stochastic radiation and broken measurements. For this purpose, we filtered out examples with radio-frequency contrast less than 50 dB. This filtering process removed 30% of the initial data. Distribution of the ACF durations after filtration is shown in Fig. 2(a). The dataset then was then divided randomly into training (80%) and testing (20%) sets. Part of the training set was used for model validation. The testing set was kept isolated from the rest during the training and optimization of the model. For ANN training we employed Adam optimization algorithm and Mean Squared Error (MSE) loss function commonly used for regression problems. To avoid overfitting, regularization and early stopping techniques were applied. After training the model, it was applied to the test set to predict durations of the ACF traces.

We found out that the model is able to predict the ACF duration with a mean absolute error near 3 ps or 4.8% mean absolute percentage error. Figure 2(b) shows measured values compared to the predicted ones. Note, that 69% and 89% of the testing samples were predicted with more than 5% and 10% relative error correspondingly. Only 3% of the testing data showed more than 20% relative error.

The obtained results were also compared with the predictions of basic linear regression and "Extreme Gradient Boosting" (XGBoost) machine learning technique [13], based on gradient boosting of regression trees [14]. The algorithm used the following parameters: the boosted trees number (150), the maximum tree depth (7) and the learning rate (0.08). The linear model achieves only 15% mean absolute percentage error, which confirms the nonlinearity of the problem. The quality of prediction drops down if duration of ACF trace exceeds 100 ps (Fig. 2(d)). The XGBoost regression demonstrated ∼5% average error, which is very close to prediction results obtained with the neural network (Fig. 2(c)). At the same time, XGBoost takes less time to be trained relative to ANN and does not require rigorous parameter settings (number of hidden layers and neurons on each layer, learning rate, etc.). In our case, the difference between the XGBoost and ANN is not significant and both methods performed well in solving the regression problem.

Table 1. Mean error of the different prediction examples

model	ACF width	RF contrast	Signal $\Delta\lambda$
ANN	4.8% (3.1 ps)	3.1% (1.9 dB)	5.8% (0.13 nm)
XGBoost	5% (3.2 ps)	3% (1.8 dB)	4.8% (0.11 nm)
Linear	15% (10.2 ps)	4% (2.3 dB)	14% (0.29 nm)

At the next stage we tried to determine the other essential characteristics of the realized pulses, such as optical spectral width ($\Delta\lambda$) and radio-frequency beating spectra contrast before propagation in fibers pool of the DFT measurement setup. it is worth noting, that the same ANN architecture and parameters

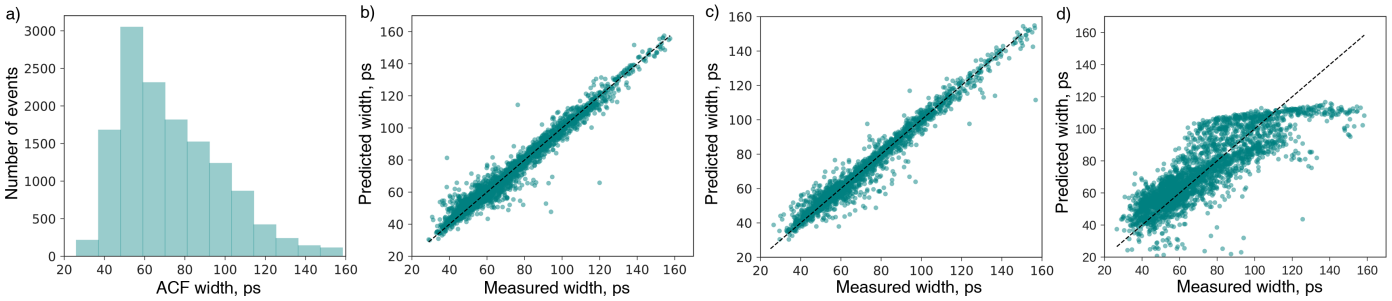

Fig. 2. (a) Distribution of the ACF durations. (b-d) Measured width of ACF traces compared to the predicted ones for the test set using the neural network (b), XGBRegressor (c) and linear regression model (d).

of xgboost as for ACF trace duration were used for prediction. Mean percentage and absolute errors of the different prediction examples obtained from each of the three models are summarized in the table 1. Therefore, the building models are able to make accurate predictions for basic characteristics of the single-pulse generation regime of the F-8 laser.

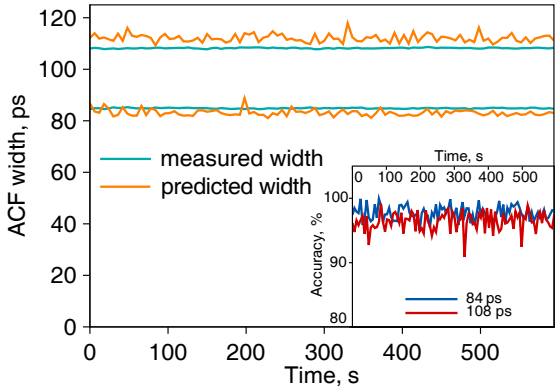

Fig. 3. Comparison of the measured and predicted ACF durations of operating laser. Inset: Accuracy of prediction.

Finally, the trained neural network was applied to operating F-8 fiber laser. We measured ACF of a pulsed regime and its DFT trace independently and calculated prediction accuracy of a pulse duration. Time series of the measured and predicted width of the ACFs, corresponding to the two mode-locked regimes with ∼84 ps and ∼108 ps output pulses, are shown in Fig. 3. Time fluctuations of the predicted width exceed fluctuations of the measured width due to difference in integration time of the autocorrelator and oscilloscope and can be attributed to fluctuations of the pulse train at the laser output. The average error maintained below 5% level during the whole measurement time (Fig. 3, inset). We tested our model on different pulsed regimes and made sure that predictions had the same degree of accuracy. Thus, DFT analysis in combination with machine learning algorithms can be used for control of the F-8 fiber laser operation, for example, for calculation of objective functions of the pulsed regimes. [15].

4. CONCLUSION

In conclusion, we demonstrated for the first time a novel method for determination of a temporal duration of the mode-locked pulses using DFT trace of pulse comb and machine learning technique. This method can be further improved, e.g. by more advanced filtering of the noisy and unstable signal generation regimes. Of course, different types of fiber lasers will generate pulses with different properties and distributions of key parameters. Their investigation will require new researching efforts and adjusting of machine learning algorithms. However, the obtained results clearly show a feasibility of accurate prediction of the basic pulse characteristics of F-8 fiber laser, i.e. temporal width, optical spectrum and radio-frequency spectrum using data extracted from the oscilloscope measurements. In other words, a single device could be used for resolving all key laser pulse parameters. Such compact and robust measuring device can be a key component for realization of feedback loop in systems that require self-starting and self-optimization.

5. FUNDING INFORMATION

This work was supported by the Russian Science Foundation (Grant No. 17-72-30006)

REFERENCES

1. R. Iegorov, T. Teamir, G. Makey, and F. Ilday, Optica **3**, 1312 (2016).
2. J. Peng and S. Boscolo, Sci. reports **6**, 25995 (2016).
3. B. Nyushkov, S. Kobtsev, A. Komarov, K. Komarov, and A. Dmitriev, JOSA B **35**, 2582 (2018).
4. S. Kobtsev, A. Ivanenko, A. Kokhanovskiy, and S. Smirnov, Laser Phys. Lett. **15**, 045102 (2018).
5. R. Woodward and E. Kelleher, Sci. reports **6**, 37616 (2016).
6. U. Andral, J. Buguet, R. S. Fodil, F. Amrani, F. Billard, E. Hertz, and P. Grelu, JOSA B **33**, 825 (2016).
7. T. Baumeister, S. L. Brunton, and J. N. Kutz, JOSA B **35**, 617 (2018).
8. C. A. Farfan, J. Epstein, and D. B. Turner, Opt. letters **43**, 5166 (2018).
9. R. Trebino, *Frequency-resolved optical gating: the measurement of ultrashort laser pulses* (Springer Science & Business Media, 2012).
10. A. Sanchez-Gonzalez, P. Micaelli, C. Olivier, T. Barillot, M. Ilchen, A. Lutman, A. Marinelli, T. Maxwell, A. Achner, M. Agåker *et al.*, Nat. communications **8**, 15461 (2017).
11. K. Goda and B. Jalali, Nat. Photonics **7**, 102 (2013).
12. M. Abadi, P. Barham, J. Chen, Z. Chen, A. Davis, J. Dean, M. Devin, S. Ghemawat, G. Irving, M. Isard *et al.*, "Tensorflow: a system for large-scale machine learning." in *OSDI*, , vol. 16 (2016), pp. 265–283.
13. T. Chen and C. Guestrin, "Xgboost: A scalable tree boosting system," in *Proceedings of the 22nd acm sigkdd international conference on knowledge discovery and data mining*, (ACM, 2016), pp. 785–794.
14. J. H. Friedman, Annals statistics pp. 1189–1232 (2001).
15. A. Kokhanovskiy, A. Ivanenko, S. Kobtsev, S. Smirnov, and S. Turitsyn, Sci. reports **9**, 2916 (2019).

FULL REFERENCES

1. R. Iegorov, T. Teamir, G. Makey, and F. Ilday, "Direct control of mode-locking states of a fiber laser," Optica **3**, 1312–1315 (2016).
2. J. Peng and S. Boscolo, "Filter-based dispersion-managed versatile ultrafast fibre laser," Sci. reports **6**, 25995 (2016).
3. B. Nyushkov, S. Kobtsev, A. Komarov, K. Komarov, and A. Dmitriev, "Soa fiber laser mode-locked by gain modulation," JOSA B **35**, 2582–2587 (2018).
4. S. Kobtsev, A. Ivanenko, A. Kokhanovskiy, and S. Smirnov, "Electronic control of different generation regimes in mode-locked all-fibre f8 laser," Laser Phys. Lett. **15**, 045102 (2018).
5. R. Woodward and E. Kelleher, "Towards 'smart lasers': self-optimisation of an ultrafast pulse source using a genetic algorithm," Sci. reports **6**, 37616 (2016).
6. U. Andral, J. Buguet, R. S. Fodil, F. Amrani, F. Billard, E. Hertz, and P. Grelu, "Toward an autosetting mode-locked fiber laser cavity," JOSA B **33**, 825–833 (2016).
7. T. Baumeister, S. L. Brunton, and J. N. Kutz, "Deep learning and model predictive control for self-tuning mode-locked lasers," JOSA B **35**, 617–626 (2018).
8. C. A. Farfan, J. Epstein, and D. B. Turner, "Femtosecond pulse compression using a neural-network algorithm," Opt. letters **43**, 5166–5169 (2018).
9. R. Trebino, *Frequency-resolved optical gating: the measurement of ultrashort laser pulses* (Springer Science & Business Media, 2012).
10. A. Sanchez-Gonzalez, P. Micaelli, C. Olivier, T. Barillot, M. Ilchen, A. Lutman, A. Marinelli, T. Maxwell, A. Achner, M. Agåker *et al.*, "Accurate prediction of x-ray pulse properties from a free-electron laser using machine learning," Nat. communications **8**, 15461 (2017).
11. K. Goda and B. Jalali, "Dispersive fourier transformation for fast continuous single-shot measurements," Nat. Photonics **7**, 102 (2013).
12. M. Abadi, P. Barham, J. Chen, Z. Chen, A. Davis, J. Dean, M. Devin, S. Ghemawat, G. Irving, M. Isard *et al.*, "Tensorflow: a system for large-scale machine learning." in *OSDI,* , vol. 16 (2016), pp. 265–283.
13. T. Chen and C. Guestrin, "Xgboost: A scalable tree boosting system," in *Proceedings of the 22nd acm sigkdd international conference on knowledge discovery and data mining,* (ACM, 2016), pp. 785–794.
14. J. H. Friedman, "Greedy function approximation: a gradient boosting machine," Annals statistics pp. 1189–1232 (2001).
15. A. Kokhanovskiy, A. Ivanenko, S. Kobtsev, S. Smirnov, and S. Turitsyn, "Machine learning methods for control of fibre lasers with double gain nonlinear loop mirror," Sci. reports **9**, 2916 (2019).